

# Electron tomography in the Scanning Electron Microscope for the investigation of biological and inorganic samples

Maurizio Donarelli,<sup>1</sup> Matteo Ferroni,<sup>1,2</sup> Luca Masini,<sup>2</sup> Vittorio Morandi,<sup>2</sup> Andrea Migliori,<sup>2</sup> Luca Ortolani,<sup>2</sup> Andrea Sanzogni,<sup>1</sup> Alberto Signoroni<sup>1</sup>

<sup>1</sup>Department of Information Engineering, University of Brescia; <sup>2</sup>CNR-Microelectronic and Microsystems Institute, Bologna, Italy

Corresponding author: Maurizio Donarelli, Department of Information Engineering, University of Brescia, Via Branze 38, 25123 Brescia, Italy. Tel. +39.030.3715877 – Fax: +39 030 2091271.  
E-mail: maurizio.donarelli@unibs.it

Key words: Electron tomography; STEM; heterostructure.

Acknowledgments: Remembering Pier Giorgio Merli after ten years from his tragic disappear, the authors are thankful for his legacy and inspiring work on image formation in the electron microscope.

The authors also acknowledge C. R. Chandraiahgari, G. De Bellis, M. S. Sarto and D. Quaglino for the supply of the samples.

## SUMMARY

This paper reports on the implementation of electron tomography in the Scanning Electron Microscope, describing its application in both physical and biological sciences. The experimental set up for tomography is described with emphasis on the scanning-transmission imaging modality, which allows one to record a series of projective images of a thin specimen. The computation of the three-dimensional arrangement of the constituents in graphene-ZnO nanorods and in collagen fibrils in dermal tissue is discussed. In addition, we show how the implementation of a compressed sensing approach can be useful to preserve nanometric resolution and overcome the limitations of the experimental strategy.

## Introduction

Tomography is a computer-assisted technique widely used in the fields of materials- and life- science to obtain a three-dimensional (3D) representation of a sample under investigation. The theoretical approach to retrieve the 3D representation of a sample starting from a series of projections was first proposed by Radon (1917) and subsequently implemented by Bracewell (1999).

The effective integration of tomography in the electron microscope (electron tomography) found the first application in biological studies in 1968, with the seminal work of De Rosier and Klug (Nobel Prize in 1982) and continues up to now to play a key role in the understanding the structure-property relationship for the biological function of cellular structures and the investigation of macromolecular assembling (J. Dubochet, J. Franck, and R. Henderson - Nobel Prize for Chemistry 2017 for “developing cryo-electron

Received for publication: 21 February 2018. Accepted for publication: 13 March 2018.

©Copyright M. Donarelli *et al.*, 2018

Licensee PAGEPress, Italy

microscopie 2018; 29:7370

doi:10.4081/microscopie.2018.7370

This article is distributed under the terms of the Creative Commons Attribution Noncommercial License (by-nc 4.0) which permits any noncommercial use, distribution, and reproduction in any medium, provided the original author(s) and source are credited.

*microscopy for the high-resolution structure determination of biomolecules in solution*)”.

In materials science, the continuously-growing interest on nanosized heterostructures, low dimensional materials and highly engineered materials (blended or reinforced polymers, porous foams and scaffolds, catalysts, bio-inspired materials) calls for a volumetric reconstruction of the spatial arrangement of constituents, challenging the operative workflow to attain nanometric resolution.

Electron tomography (ET) is commonly carried out in Transmission Electron Microscope (TEM), operating in different modes: Bright-Field imaging and Cryo-TEM for biological non-crystalline and frozen-hydrated samples, while High-Angle-Annular-Dark-Field (HAADF) Scanning-TEM (STEM) plays a major role in physical sciences (Ercius *et al.*, 2015). In HAADF-STEM, in particular, the electron beam is focused at the sample and scanned over a regular raster to record an image modulated by the intensity of the signal for incoherently-scattered electrons. A detector collects the transmitted electrons to form a two-dimensional (2D) image, which is a projection, at a given angle, of the 3D sample. In the single-axis projection scheme, the sample is rotated around the eucentric axis of the sample holder and a series of 2D projections of the specimen can be recorded. For a complete sampling, the tilting range should extend from  $-90^\circ$  to  $+90^\circ$ .

The Fourier slice theorem (or projection theorem) is the basis of 3D reconstruction. The series of real space projections recorded at different tilt angles is Fourier transformed and determines a radial sampling of the 3D Fourier transform of the object. After that, the inverse Fourier transform is carried out in order to obtain the tomogram of the sample (Crowther *et al.*, 1970). A good reconstruction should be artefact-free and suitable for a quantitative analysis of the sample under investigation. Unfortunately, this is not always possible, due to geometric and exposure time limitations in the experimental recording of the projections. Geometric limitations result in a “missing wedge”, *i.e.* the angular range not accessible for the recording of the projection series, due to the shape of the sample-holder or of the sample itself. Limitation in the electron dose is very important especially for biological samples, which can be damaged by the prolonged exposure to electron beam. Two approaches can be followed to improve the reconstruction quality. The first deals with the projections’ acquisition scheme, for example using double tilt-axis or conical tomography, as well as special sample holders, fast detectors and particular sample preparation (Zampighi *et al.*, 2005, 2008; Tong and Midgley, 2006; Arslan *et al.*, 2006; Migunov *et al.*, 2015; Palmer and Löwe, 2014). The second approach deals with the processing of the projection images. A tomogram refinement can be achieved through iterative reconstruction techniques, like

Simultaneous Iterative Reconstruction Technique (SIRT), Algebraic Reconstruction Technique (ART), Ordered-Subset Algebraic Reconstruction Technique (OS-ART) and Discrete-ART (DART) (Matej *et al.*, 2004; Batenburg *et al.*, 2009; Batenburg and Sijbers, 2011; Wang and Jiang, 2004). A prior knowledge of some characteristics of the sample can also be exploited in order to refine the 3D reconstruction. The existence of a sparse and compressible representation of the signal, known *a priori*, is the basis of the Compressed Sensing (CS) technique (Leary *et al.*, 2013; Thomas *et al.*, 2013).

In the present work, we show that the tomographic approach can be implemented in the SEM platform, exploiting the capability of the scanning-transmission imaging mode. This mode, referred as Transmitted SEM (T-SEM) or low-energy STEM is an effective counter part of the HAADF-STEM mode.

We report the experimental setup for ET in SEM and the 3D reconstruction of a graphene-ZnO nanorods and nanoparticles hybrid structure. Furthermore, we show that the compressed sensing algorithmic approach can be successfully used to reconstruct a biological sample, starting from a limited number of projections and without any significant loss of information.

## Materials and Methods

### Set up for tomography

A ZEISS-LEO 1525 SEM, operated at the University of Brescia, has been used for imaging of a graphene-ZnO nanoparticles sample; in addition, a ZEISS-LEO 1530 SEM, operated at the Bologna Section of IMM-CNR, was similarly configured for imaging of a stained thin section of biological tissue (human derma). In both equipments, the transmitted electrons were collected by a Si-based detector, designed and fabricated at IMM-CNR for the purpose, constituted of five independently-operable sectors. Depending on the configuration of the detector’s sections, a bright field (BF) or a dark field (DF) image of the thin sample were recorded. The STEM signal, collected by the detector, is based on the angular distribution of the forward scattered electron. The impinging electrons energies used in this work are 27 kV for the graphene-ZnO nanorods and nanoparticles structure (Ferroni *et al.*, 2017) and 30 kV for the biological sample. As introduced in the previous section, for the 3D reconstruction of a volume, a series of 2D projections of the investigated samples have to be acquired. To do so, the samples are prepared on a standard TEM grid and are mounted on a rotating holder. Figure 1 shows the STEM set-up for the tomography, and highlights the basic parameters of the imaging configuration. The sample is rotated around its

eucentric axis and the detector beneath it is used to record STEM images of the sample, obtaining the series of the projections of the sample.

### Samples fabrication

Graphene flakes have been fabricated by solvo-thermal exfoliation method and ZnO nanorods (NR) have been grown *in situ* by aqueous hydrothermal method (Chandraiahgari *et al.*, 2016). After that, the heterostructure have been drop cast on a TEM grid for the observation.

A collagen specimen from human dermal tissue has been used as a representative biological sample. The sample has been fixed in 2.5% glutaraldehyde and 1% osmium tetroxide, dehydrated, and embedded in Spurr resin. Ultramicrotomy has been performed in order to obtain 0.7  $\mu\text{m}$  thick sample (Ferroni *et al.*, 2016).

## Results

### Graphene-ZnO heterostructure 3D reconstruction

The SEM secondary electrons image (recorded by Everhart-Thorley detector) of the graphene-ZnO heterostructure is reported in Figure 2-left. The ZnO nanostructures are clearly visible (they are the bright features in the image). On the contrary, the zinc oxide nanostructures appear dark in the BF-STEM image reported in Figure 2-right, due to the fact that are thicker and heavier than the graphene flake.

The best imaging condition for this sample for the acquisition of a series of projections at different tilt angles is the DF-STEM mode. In this case, no mass-thickness contrast inversion has been noticed during the tilting of the sample between  $-50^\circ$  and  $+50^\circ$ . Furthermore, the DF mode enables to obtain images with ZnO nanostructures clearly distinguish-

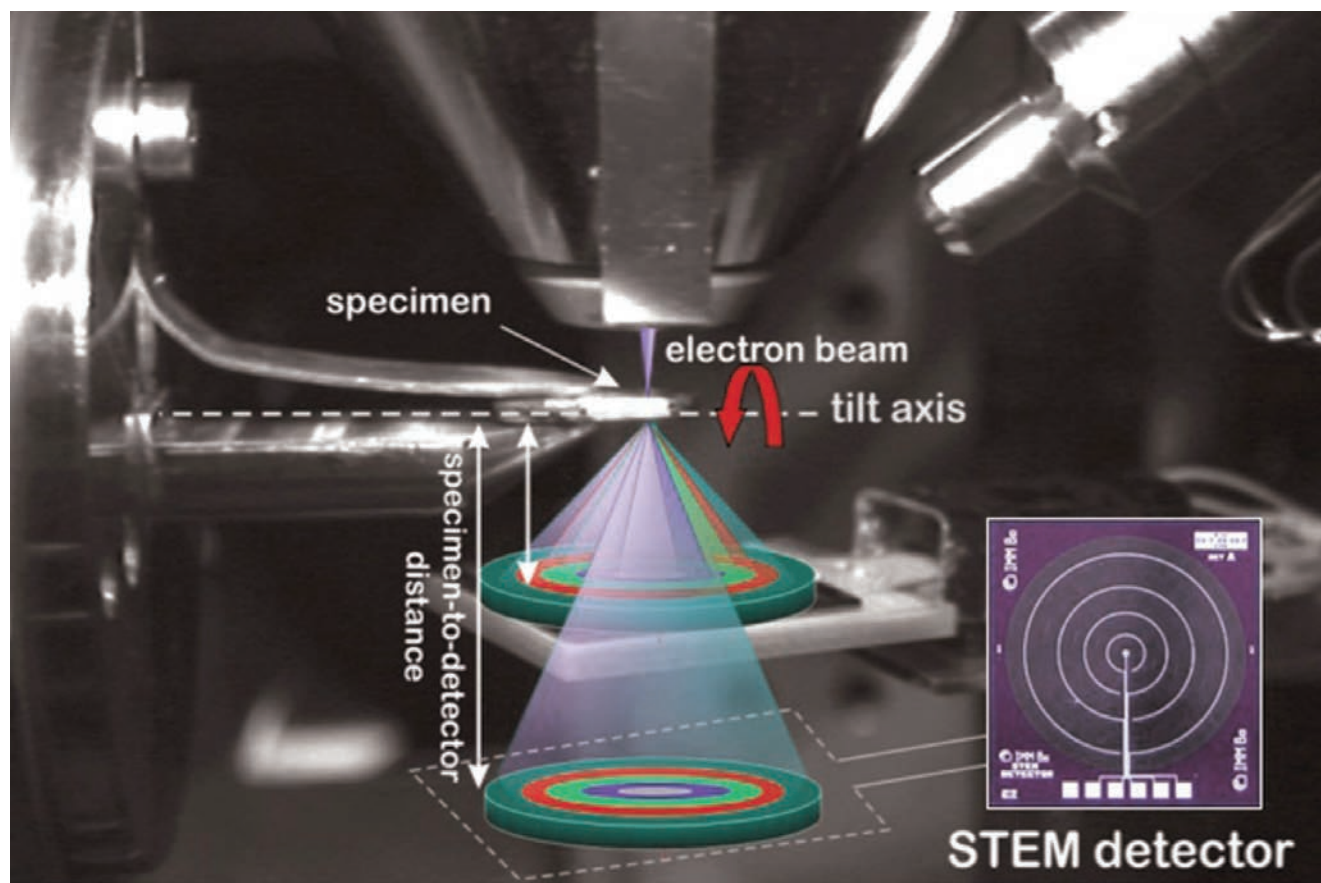


Figure 1. Schematic layout of the tomography setup in the ZEISS-LEO 1530 SEM at CNR-IMM. The inset highlights the circular sectors of the Si-based STEM detector.

able from the graphene matrix. DF-STEM projections of the sample, at different tilt angles are reported in Figure 3.

The projection images have been recorded at tilt angles ranging from  $-50^\circ$  to  $+50^\circ$ , with a  $2^\circ$  step. The acquisition time was 2.6 s at 100 ms dwell.

The 3D reconstruction can be affected by artefacts, mainly coming from the “missing wedge” and the misalignment of the projection images. While the presence of the “missing wedge” is almost unavoidable, due to the geometry of the setup, which limits the investigated tilting range, the misalignment of the projection images can be overcome by several procedures. Here, we have adopted an alignment procedure based on the cross-correlation of the projection images. We have aligned the projection images first using a Gatan free software ([www.gatan.com](http://www.gatan.com)), followed by a macro implemented in TomoJ-ImageJ (Sanchez Sorzano *et al.*,

2009). In this way, the projection images are well aligned, and considering that the measured distances of the particles lying on the TEM grid from axis (estimated image-by-image) follow a cosinusoidal behavior, the distance vs. tilt angle curve can be fitted to obtain a correct estimation of the position of the tilt axis. An OS-ART algorithm, implemented in TomoJ (Messaoudii *et al.*, 2007), and iterated 50 times, has been used to reconstruct the 3D image from the 51 projection images. The thickness of the 3D reconstruction has been set to 50 pixels. In Figure 4, we report the 3D reconstruction of the graphene-ZnO heterostructure.

The light blue regions of the image are the ZnO nanorods and/or nanoparticles. It is worth noting that the presence of a “missing wedge” results in the elongation of reconstructed nanostructures along the  $z$ -direction (*i.e.*, the direction perpendicular to the plane containing the tilt axis).

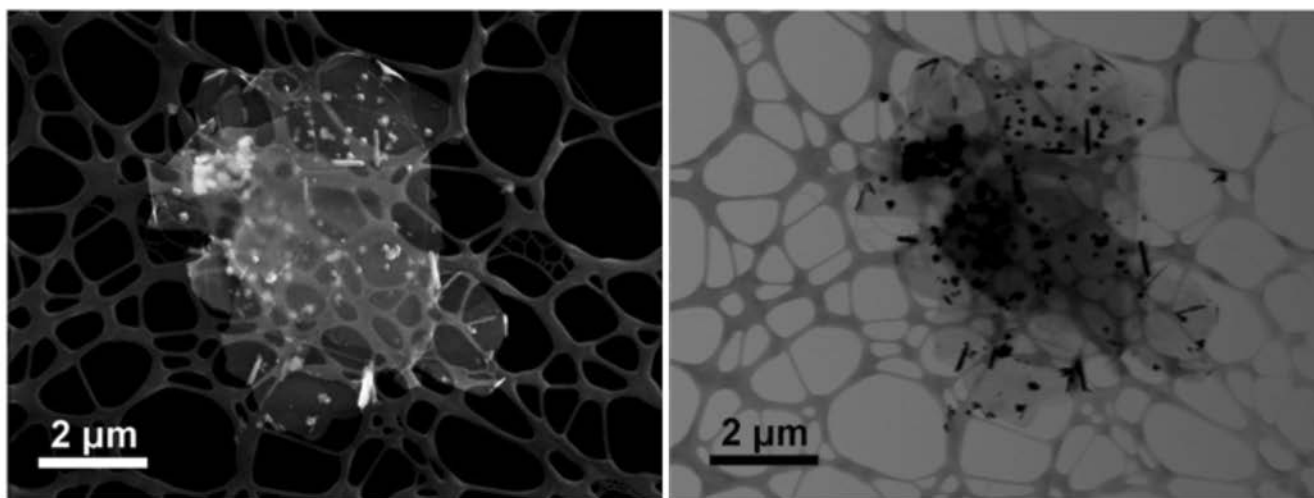


Figure 2. Left: secondary electrons (Everhart-Thorley detector) SEM image of the graphene-ZnO heterostructure (accelerating voltage 20 kV). Right: image of the same heterostructure obtained in DF-STEM mode (accelerating voltage 27 kV).

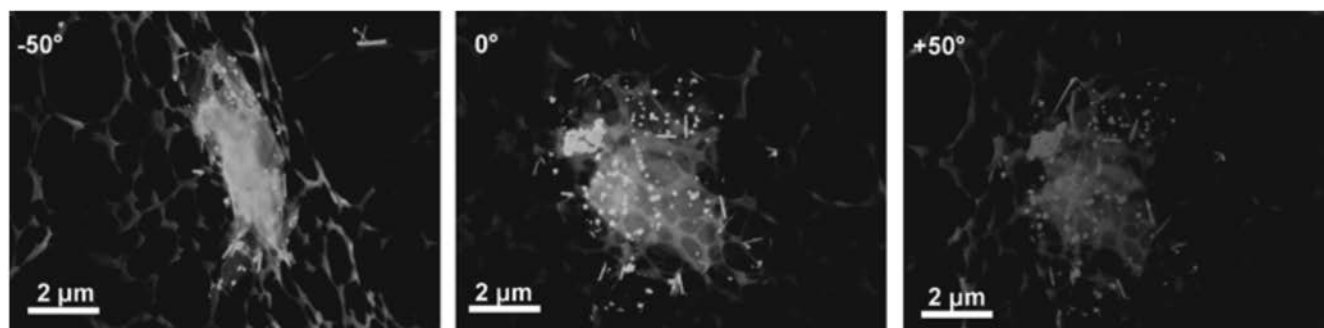


Figure 3. DF-STEM projections of the investigated sample at different tilt angles.

### ET and CS for the 3D reconstruction of a collagen specimen

In the previous section, the 3D reconstruction of a materials science sample has been reported. The main problems in the reconstruction process lie on registration of the images and on the limited number of projections that can be used. In the case of biological sample, one has to consider also the effect of the incident electron beam, which can damage the specimen. Here, we report the 3D reconstruction of a specimen featuring collagen fibrils in dermal tissue, and how the CS technique can be useful to limit the number of projections needed to obtain a good 3D tomogram of the sample. The experimental setup and the projections acquisition procedure for the collagen specimen is basically the same of the one reported in the previous sections for the graphene-ZnO sample. The sample has been tilted to obtain a series of projection images (91, from  $-50^\circ$  to  $+40^\circ$ , with  $1^\circ$  step, 30 kV accelerating voltage) in DF-STEM mode. A SEM image of the sample is reported in Figure 5.

The tomogram has been calculated by using all of the 91 projection images and refined by a CS technique (Figure 6a). The use of CS becomes important when the number of the projections is significantly decreased. It can be observed

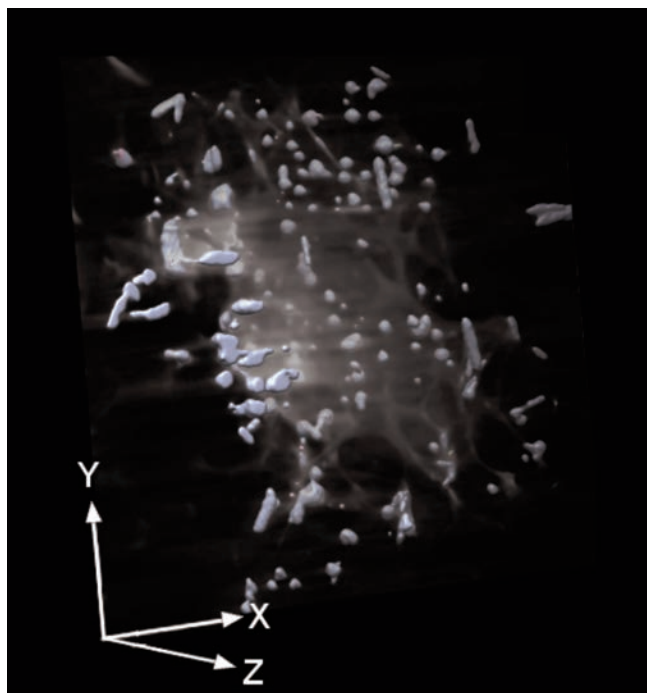


Figure 4. 3D reconstruction of the graphene-ZnO heterostructure.

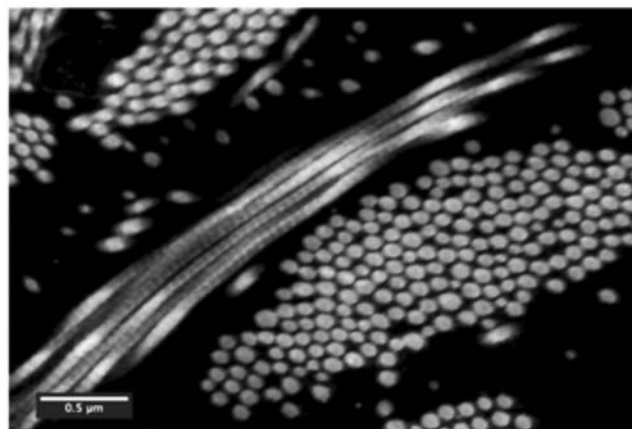


Figure 5. SEM image of the collagen sample (accelerating voltage 15 kV). Adapted from Ferroni *et al.*, *Sci. Rep.* 2016;6:33354, with permission.

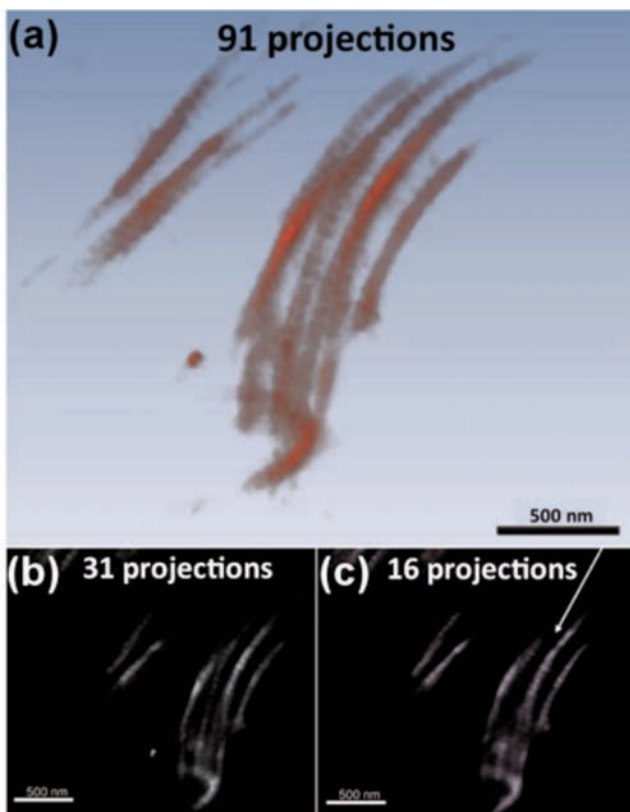


Figure 6. a) CS refined tomogram of the collagen bundle sample, using all the 91 projection images. b) CS refined tomogram of the sample, using only 31 projections; no significant loss of information can be noticed. c):CS refined tomogram of the sample, using 16 projections; the arrow indicates a missing fibril. Adapted from Ferroni *et al.*, *Sci. Rep.* 2016;6:33354, with permission.

that, even if the number of projections is decreased at 31, the CS refined tomogram is good enough to clearly see the striation of the collagen bundles, without any significant loss of information (Figure 6b). Using only 16 projections and CS refinement, some particulars of the tomogram are lost: the arrow in Figure 6c indicates a fibril missing in the tomogram. With the help of CS technique, the reconstruction of biological samples, from a low number of projections, can be achieved, with a resolution of 20-60 nm and a reconstructed volume of the order of  $1 \mu\text{m}^3$ .

## Conclusions

Electron tomography in SEM platform is a viable technique to obtain 3D information about thin biological and material science samples and complements the serial-sectioning imaging method. The projection images are obtained with SEM operating in the transmission mode, at standard magnification. The reconstruction can achieve nanometric resolution and volumes up to  $1 \mu\text{m}^3$  can be reconstructed. Furthermore, the compressed sensing technique allows to refine the reconstruction and to reduce the number of projections required to obtain a good 3D reconstruction, especially for biological samples, which can be affected by the incident electron beam.

## References

- Arslan I, Tong J, Midgley PA. Reducing the missing wedge: High-resolution dual axis tomography of inorganic materials. *Ultramicroscopy* 2006;106:994-1000.
- Batenburg KJ, Bals S, Sijbers J, Kübel C, Midgley PA, Hernandez JC, et al. 3D imaging of nanomaterials by discrete tomography. *Ultramicroscopy* 2009;109:730-40.
- Batenburg KJ, Sijbers J. DART: a practical reconstruction algorithm for discrete tomography. *IEEE Trans Image Process* 2011; 20:2542-53.
- Bracewell RN. *The Fourier transform and its applications*, 3rd e. McGraw-Hill, New York; 1999.
- Chandraiahgari CR, De Bellis G, Balijepalli SK, Kaciulis S, Ballirano P, Migliori A, et al. Control of the size and density of ZnO-nanorods grown onto graphene nanoplatelets in aqueous suspensions. *RSC Adv* 2016; 86:83217-25.
- Crowther RA, De Rosier DJ, Klug A. The reconstruction of a three-dimensional structure from projections and its application to electron microscopy. *Proc R Soc London Ser A* 1970;317:319-40.
- Ercius P, Alaidi O, Rames MJ, Ren G. Electron tomography: A three-dimensional analytic tool for hard and soft materials research. *Adv Mater* 2015;27:5638-63.
- Ferroni M, Donarelli M, Morandi V, Migliori A, Ortolani L, Signoroni A, et al. SEM tomography for the investigation of hybrid structures. *J Phys Conf Ser* 2017;902:012031.
- Ferroni M, Signoroni A, Sanzogni A, Masini L, Migliori A, Ortolani L, et al. Biological application of compressed sensing tomography in the scanning electron microscope. *Sci Rep* 2016;6:33354.
- Leary R, Saghi Z, Midgley PA, Holland DJ. Compressed sensing electron tomography. *Ultramicroscopy* 2013;131:70-91.
- Matej S, Fessler JA, Kazantsev IG. Iterative tomographic reconstruction using Fourier-based forward and back-projectors. *IEEE Trans Med Imag* 2004;23:401-12.
- Messaoudii C, Boudier T, Sanchez Sorzano CO, Marco S. TomoJ: tomography software for three-dimensional reconstruction in transmission electron microscopy. *BMC Bioinformatics* 2007;8:288.
- Migunov V, Ryll H, Zhuge X, Simson M, Strüder L, Joost Batenburg K, et al. Rapid low dose electron tomography using a direct electron detection camera. *Sci Rep* 2015;5:14516.
- Palmer CM, Löwe J. A cylindrical specimen holder for electron cryo-tomography. *Ultramicroscopy* 2014;137:20-9.
- Radon J. [Über die Bestimmung von Funktionen durch ihre Integralwerte längs gewisser Mannigfaltigkeiten]. [Article in German]. *Ber Sächs Akad Wiss* 1917;69:262-7.
- Sanchez Sorzano CO, Messaoudii C, Elbauer M, Bilbao-Castro JR, Hegeri R, Nickell S, et al. Marker-free image registration of electron tomography tilt-series. *BMC Bioinformatics* 2009;10:124.
- Thomas JM, Leary R, Midgley PA, Holland DJ. A new approach to the investigation of nanoparticles: Electron tomography with compressed sensing. *J Colloid Interface Sci* 2013;392:7-14.
- Tong J, Midgley PA. A novel dual-axis reconstruction algorithm for electron tomography. *J Phys Conf Ser* 2006; 26:33-6.
- Wang G, Jiang M. Ordered-subset simultaneous algebraic reconstruction techniques (OS-SART). *J Xray Sci Technol* 2004;12:169-77.
- Zampighi GA, Fain N, Zampighi LM, Cantele F, Lanzavecchia S, Wright EM. Conical electron tomography of a chemical synapse: polyhedral cages dock vesicles to the active zone. *J Neurosci* 2008;28:4151-60.
- Zampighi GA, Zampighi L, Fain N, Wright EM, Cantele F, Lanzavecchia S. Conical tomography II: A method for the study of cellular organelles in thin sections. *J Struct Biol* 2005;151:263-24.